

Elastic modulus of biomedical titanium alloys by nano-indentation and ultrasonic techniques—A comparative study

P. Majumdar*, S.B. Singh, M. Chakraborty

Department of Metallurgical and Materials Engineering, Indian Institute of Technology, Kharagpur 721302, India

Received 13 November 2007; received in revised form 18 December 2007; accepted 19 December 2007

Abstract

The elastic modulus of near β and β titanium alloys was measured by nano-indentation and ultrasonic techniques. The data obtained from both the experiments were analyzed and compared with each other. The effects of composition and heat treatment on elastic modulus of the material are discussed. The elastic modulus of β Ti–35Nb–5.7Ta–7.2Zr (TNTZ) was found to be half of the elastic modulus of the titanium. Near β Ti–13Zr–13Nb (TZN) alloy hot worked at 800 °C and solution treated at 800 °C followed by water quenching also showed low elastic modulus value. The accuracy of these two elastic modulus measurement techniques is discussed in terms of microstructures.

© 2007 Elsevier B.V. All rights reserved.

Keywords: Elastic modulus; Nano-indentation; Ultrasonic technique; Titanium alloys

1. Introduction

Titanium and its alloys are commonly used as implant materials because of their high strength to density ratio, superior biocompatibility and corrosion resistance, good mechanical properties and low elastic modulus [1,2]. $\alpha + \beta$ type Ti–6Al–4V has been the main biomedical titanium alloy for a long period [3]. V-free titanium alloys like Ti–6Al–7Nb and Ti–5Al–2.5Fe have been recently developed because toxicity of V has been reported [4]. Moreover, Kawahara [5] has reported that metallic Al, V and Fe have higher cytotoxicity. Similarly, near equiatomic TiNi alloys have been in clinical practice for several years because of their special mechanical properties of shape memory effect and superelasticity. However, recently Ni has been classified as incompatible and toxic [6].

The elastic modulus of Ti and $\alpha + \beta$ Ti alloys (100–110 GPa) is much smaller than stainless steel (210 GPa), but it is significantly higher than that of bone tissue which has elastic modulus in the range of 10–40 GPa. This gives rise to the so-called ‘stress shielding’ effect that can cause bone resorption and loosening of implant [3,7]. This problem can be minimized if alloy with elastic modulus closer to that of the bone is used.

Recent research has attempted to overcome the long-term health problem caused by the release of the toxic ions from the alloys as well as the stress shielding effect. New low elastic modulus near- β and metastable- β titanium alloys containing only non-toxic metallic alloying elements such as Nb, Ta, and Zr, etc., with excellent mechanical properties are being developed as potential implant material [1]. Zr is added to increase the strength, while Ta is expected to improve corrosion resistance and mechanical performance [8]. Nb is added as a β stabilizing element and it increases hot workability also [9]. In view of the above considerations, extensive work has been carried out on near β and metastable β alloys containing Nb, Zr, Ta, Mo, etc. [7,10–21]. Some recently developed alloys of this family include Ti–12Mo–6Zr–2Fe, Ti–15Mo–5Zr–3Al, Ti–15Mo–3Nb–3O, Ti–15Zr–4Nb–4Ta, Ti–35Nb–5Ta–7Zr, Ti–13Zr–13Nb, Ti–34Nb–9Zr–8Ta, Ti–13Mo–7Zr–3Fe, Ti–13Mo, Ti–7.5Mo, Ti–15Mo–5Zr–3Al, Ti–29Nb–13Zr–2Cr, Ti–29Nb–15Zr–1.5Fe, Ti–29Nb–10Zr–0.5Si, Ti–29Nb–10Zr–0.5Cr–0.5Fe and Ti–29Nb–18Zr–2Cr–0.5Si, Ti–29Nb–13Ta–4.6Zr, etc. (all in wt.%) [7,11,15,19–22].

In a multiphase alloy, the elastic modulus is determined by the modulus of the individual phases and by their volume fractions [1]. Elastic modulus is more sensitive to phase/crystal structure than to other factors [23]. Niinomi [3] has reported the elastic modulus of different grades of titanium and a number of titanium alloys. Hao et al. [1] has investigated the influence of α'' martensite on Young’s modulus and mechanical properties of

* Corresponding author. Tel.: +91 3222 283290; fax: +91 3222 282280.

E-mail addresses: pallab@metal.iitkgp.ernet.in, m.pallab@gmail.com (P. Majumdar).

forged Ti–29Nb–13Ta–4.6Zr (wt.%) alloy and concluded that the Young's modulus of α' martensite is comparable with β phase. Saito et al. [24] have reported that cold working substantially decreases the elastic modulus and increases the yield strength of Ti–23Nb–0.7Ta–2Zr–O alloy, though the reasons for this decrease in the elastic modulus has not been discussed in detail. Munuera et al. [25] have investigated the nanoscale surface elasticity of three different titanium alloys (Ti–7Nb–6Al, Ti–13Zr–13Nb and Ti–15Zr–4Nb) in their as received state and after oxidation treatment using force microscopy mode in scanning force microscopy and reported that the Young's modulus of the sample surface was below 65 GPa and was as low as 20 GPa for some oxidized samples. The values were related to the ratio of the amount of α and β phases in the as received samples as well as to different chemical composition of the outer layers obtained after different oxidation treatment.

With the above background in mind, present investigation was undertaken to prepare and characterize 'near β ' and 'metastable β ' titanium alloys with no toxic alloying elements. Particular emphasis was laid on measuring the elastic modulus of the alloys and correlate it with the microstructure. The elastic modulus of the alloys was measured by ultrasonic method as well as by nano-indentation technique and the values obtained from these two techniques are compared in the light of microstructural variations. In addition, the elastic modulus of cp-Ti was also measured for comparison of the elastic modulus of various phases. Cp-Ti is expected to show a homogenous microstructure and therefore it was also used as a 'standard' material to examine the effectiveness of nano-indentation technique to measure the elastic modulus.

1.1. Measurement of modulus of elasticity

Young's Modulus of Elasticity is defined as the ratio of stress (force per unit area) to corresponding strain (deformation) in the elastic region of deformation of a material loaded under tension or compression. This basic material property is of interest in many manufacturing and research applications and is related to the atomic bonding of the materials. In case of biomaterials for load bearing applications, the elastic modulus is an important parameter. The stiffness mismatch between implant material and surrounding bone leads to 'stress shielding' of the bone. Higher stiffness or Young modulus of the implant will result in a greater amount of bone loss, bone fracture and loss of bone interface. Also, loss of bone due to stress shielding effects makes revision surgeries more difficult. Finite element analysis has suggested that a low elastic modulus hip prosthesis can stimulate better bone growth by distributing the stress to the adjacent bone tissue [26–29]. The elastic modulus of the materials can be determined by different methods, such as ultrasonic and nano-indentation techniques.

Nano-indentation is a technique for determining both the elastic and plastic properties of the materials at a nanoscale level in a single experiment where no special sample preparation is required (however, a good surface finish is needed). In nano-indentation, the indentation process is continuously monitored with respect to force, displacement and time. The reduced elastic

modulus, E_r , is defined as [30,31]:

$$E_r = \frac{\sqrt{\pi}}{2C} \frac{1}{\sqrt{A_c}} \quad (1.1)$$

where A_c is the projected contact area and C is the contact compliance between the indenter and the sample, equal to the tangent to the force–displacement curve during unloading at maximum load F_{\max} after correction for frame compliance:

$$C = C_t - C_f = \frac{dh}{dF} \quad (1.2)$$

where C_t is the total compliance, C_f the frame compliance, F the force and h is the displacement.

Finally,

$$\frac{1}{E_r} = \frac{1 - \nu_s^2}{E_s} + \frac{1 - \nu_i^2}{E_i} \quad (1.3)$$

where ν_s and ν_i , E_s and E_i are Poisson's ratios and elastic moduli of the sample and indenter, respectively.

Velocity of the ultrasonic waves in a solid medium is directly related to the elastic properties and density of the material. The elasticity of the material delays the transmission of wave and introduces a time delay, *i.e.* a phase lag. When the frequency of the wave is higher than the audible range, it is called elastic wave or ultrasound. Two types of vibration-induced deformation resulting in compression or shear are generally possible in an infinite medium. These are associated with two modes of elastic wave propagation, *i.e.* longitudinal waves, where particles are displaced along the direction of propagation, and transverse or shear waves, where the particles are displaced perpendicular to the direction of propagation. The velocity of propagation of the elastic waves in a body is characteristics of the material [32].

Ultrasonic waves are generated in the material by a transmitter oscillating at the desired waveform and frequency, with collection by a detector. Ultrasonic velocity changes have been determined by time-of-flight measurements using a pulse-echo method. The relationships between ultrasonic velocity and the elastic properties of materials are given below [33–35].

Young's modulus (E) is expressed as

$$E = \frac{\rho V_S^2 (3V_L^2 - 4V_S^2)}{V_L^2 - V_S^2} \quad (1.4)$$

Shear modulus (G) is the ratio of shearing stress τ to shearing strain γ within the proportional limit of a material and is expressed as

$$G = \rho V_S^2 \quad (1.5)$$

whereas, Poisson's ratio ν is the ratio of transverse contraction strain to longitudinal extension strain in the direction of stretching force and is expressed as

$$\nu = \frac{(1/2)(V_L^2 - 2V_S^2)}{V_L^2 - V_S^2} \quad (1.6)$$

In the above set of equations, V_L and V_S are the ultrasonic longitudinal and shear wave velocities, respectively, and ρ is the density of the material.

2. Experimental

Near β Ti–13Zr–13Nb (TZN) and β Ti–35Nb–5.7Ta–7.2Zr (TNTZ) alloys (compositions in wt.%) were prepared by arc melting with a non-consumable tungsten electrode in a vacuum arc melting unit supplied by *Vacuum Techniques Pvt. Ltd., Bangalore*. The melting chamber was first evacuated to less than 5×10^{-6} mbar and then flushed with high purity argon and evacuated again; the chamber was finally back-filled with the same gas before melting. Prior to melting of the alloys, titanium was melted as a getter in the furnace. The ingots were turned over and remelted at least six times in order to attain homogeneity in composition and microstructure. The TNTZ alloy ingot was hot rolled giving 40–50% deformation at 850 °C and then air cooled to room temperature. The deformed samples were further solution treated at 800 °C for 1 h followed by water quenching (WQ). The TZN alloy was hot rolled giving 30–40% deformation at two different temperatures (800 and 650 °C) and then air cooled to room temperature. It has been reported that the β transus temperature of the Ti–13Zr–13Nb alloy is 735 °C [14]. The hot rolling temperatures were selected in such a way that it was above the β transition temperature in one case (800 °C) and below that temperature in another (650 °C). The samples hot worked at 800 °C were solution treated at 800 °C and those hot worked at 650 °C were solution treated at 700 °C for 1 h in dynamic argon atmosphere followed by furnace cooling (FC) and water quenching (WQ). Elastic modulus of as received commercially pure Ti (cp-Ti, grade 4) was also measured for comparison.

Room temperature X-ray diffraction analysis was carried out in a *Philips, Holland, PW 1710 X-ray Diffractometer* with Cu $K\alpha$ radiation at 40 kV and 20 mA. The scanning rate was kept at $3^\circ-2\theta/\text{min}$, from $2\theta = 20^\circ$ to 100° .

Optical microscopy was carried out on Leica DFC320 image analyzer (Model: Q550IW) interfaced with Leica Q-win V3 Image analysis software. Optical micrographs of the metallographically polished samples were taken using a digital camera attached to the microscope and interfaced with a computer. Samples were prepared by following standard metallographic technique. The polished samples were etched with Kroll's reagent (10 vol.% HF and 5 vol.% HNO₃ in water).

Nano-indentation equipment is used to investigate mechanical properties of materials by indenting the test material with

a diamond tip to a certain depth (nano-meter range) while measuring the force–displacement response. In the present investigation, elastic modulus of cp-Ti and heat-treated titanium alloys was directly measured by nano-indentation technique on a *Nano Indenter[®] XP, MTS Systems Corporation, USA* by using a Berkovich diamond indenter. Two samples were tested for each composition and heat treatment condition. Indentations were sufficiently spaced so that the indentation behaviour was not affected by the presence of adjacent indentations. The elastic modulus was calculated automatically during unloading by employing the test software using Eqs. (1.1)–(1.3).

The other experimental conditions were:

- (i) Depth limit: 3000 nm.
- (ii) Strain rate target: 0.05 s^{-1} .
- (iii) Maximum calculation depth: 2500 nm.
- (iv) Minimum calculation depth: 1000 nm.

The elastic modulus of the heat-treated samples was measured by ultrasonic method on an ultrasonic velocity gauge, *35 DL, Panametric, USA*. A normal incident probe, model M110, 5 MHz and a shear probe, model V221, 5 MHz were used for the measurement of normal and shear velocities of the wave, respectively. The density of the samples was measured using Archimedes principle; for each composition and heat treatment condition, at least five samples were measured.

3. Results and discussion

3.1. Microstructure and XRD

The microstructure of cp-Ti consisted of single-phase α grains (Fig. 1a). The XRD analysis also confirmed the same (Fig. 1b). The microstructure of the TNTZ alloy deformed (40–50% reduction) at 850 °C and then solution treated at 800 °C followed by WQ shown in Fig. 2a, clearly reveals the presence of equiaxed β grains. The XRD patterns (Fig. 2b) also suggested that the microstructure consists of β phase. Although fine α or ω phase is considered to exist in the heat-treated TNTZ alloy, its presence could not be detected by XRD. Though similar results have been reported elsewhere [18], a detailed characterization is necessary for better understanding of the microstructure.

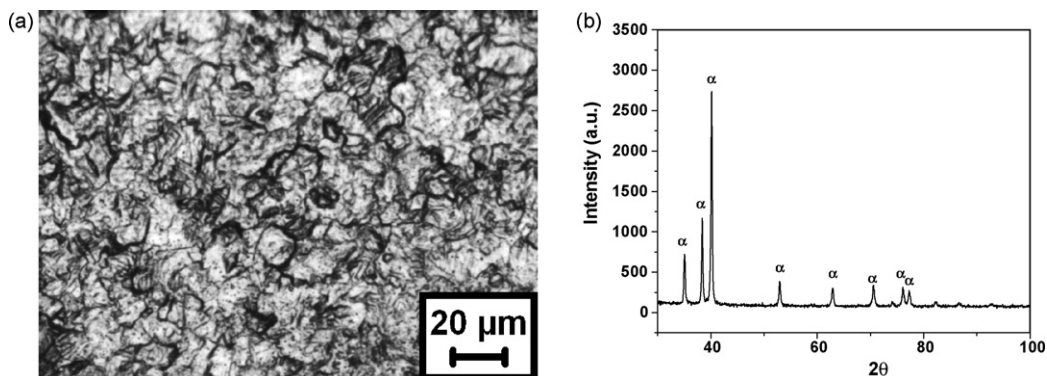


Fig. 1. (a) Microstructure and (b) X-ray diffraction pattern of the cp-Ti.

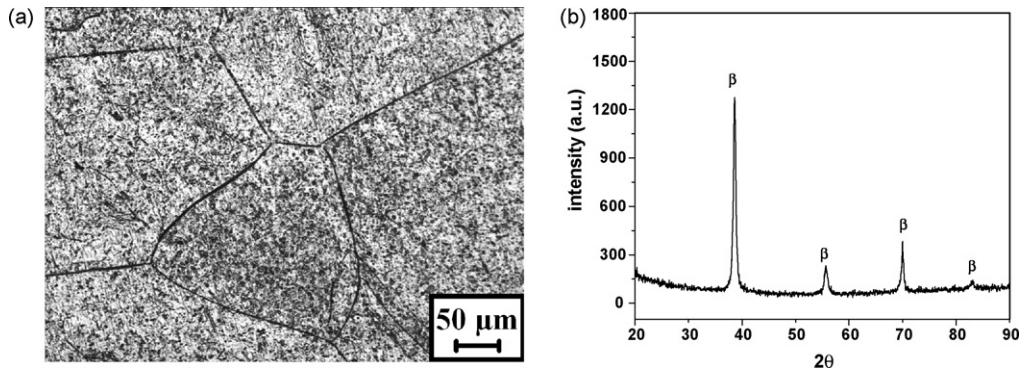


Fig. 2. (a) Microstructure and (b) X-ray diffraction pattern of the TNTZ alloy deformed at 850 °C and solution treated at 800 °C for 1 h followed by water quenching.

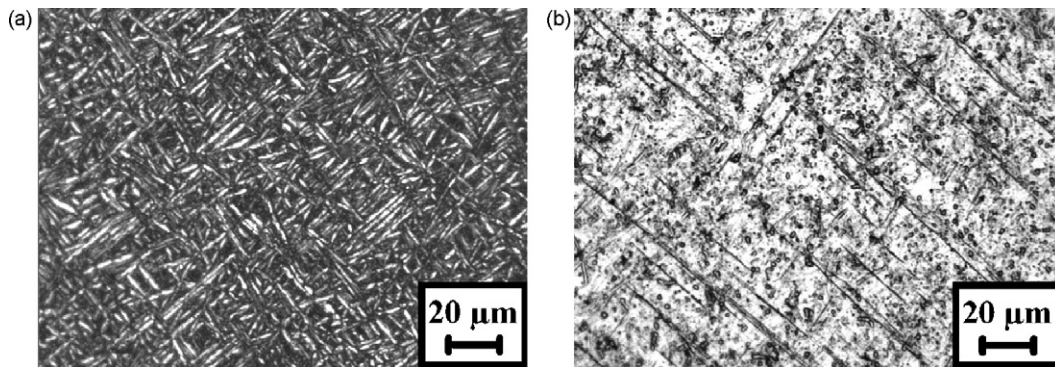


Fig. 3. Microstructures of the TZN alloy deformed at 800 °C and solution treated at 800 °C for 1 h followed by (a) furnace cooling and (b) water quenching.

The microstructure of the TZN alloy deformed (30–40% reduction) at 800 and 650 °C (above and below the β transition temperature, respectively) followed by different sets of heat treatment conditions is shown in Figs. 3 and 4. Samples deformed above β transus, *i.e.* at 800 °C and heat treated at 800 °C followed by furnace cooling (FC) (Fig. 3a) showed a basket-wave structure formed from prior β grains. The water quenching (WQ) from 800 °C exhibited martensite (α') structure with some amount of β (Fig. 3b).

The microstructure of the samples deformed below the β transus, *i.e.* at 650 °C and then solution treated at 700 °C for 1 h followed by FC and WQ is shown in Fig. 4a and b. The microstructure of furnace cooled sample consisted of equiaxed primary α and transformed β . The

water quenched sample showed globular α and martensite (α'')/elongated α dispersed on a very fine scale. As explained by Geetha et al. [14], it is expected that the α' martensite (hexagonal) is present in the sample water quenched from 800 °C (β solution treatment conditions) whereas α'' martensite (orthorhombic) is present when quenching from 700 °C ($\alpha + \beta$ solution treatment conditions). Quenching from the two-phase region causes the enrichment of Nb in the β phase due to partitioning effect of the alloying element and hence changes the structure of the martensite from hexagonal to orthorhombic [14]. Phase constituents of the heat-treated samples were also identified from the X-ray diffraction as shown in Fig. 5. A detailed description of the effect of heat treatment of the TZN alloy on its microstructure can be found elsewhere [36].

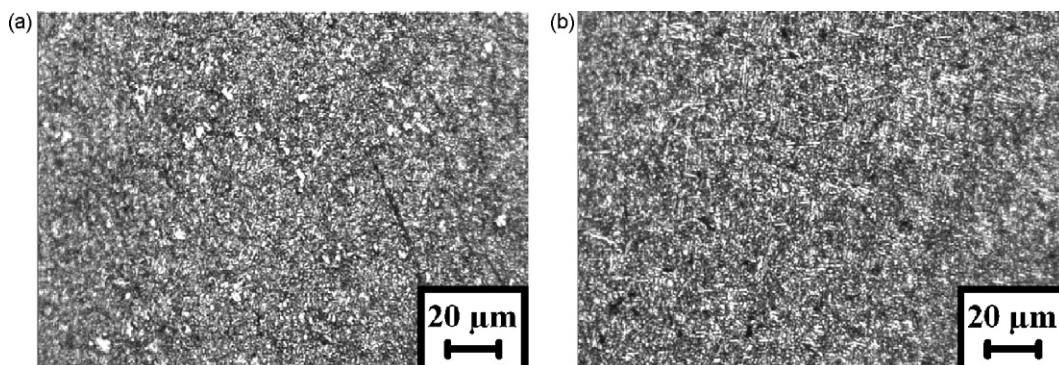


Fig. 4. Microstructures of the TZN alloy deformed at 650 °C and solution treated at 700 °C for 1 h followed by (a) furnace cooling and (b) water quenching.

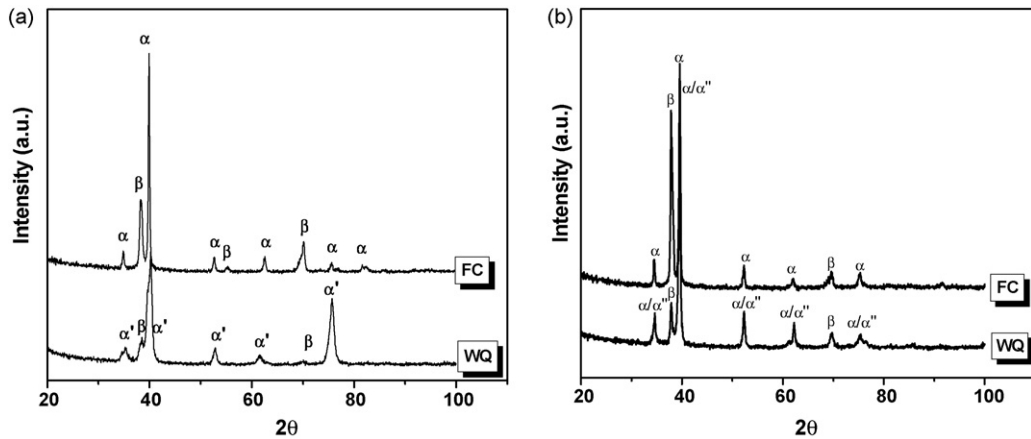


Fig. 5. XRD pattern of Ti–13Zr–13Nb alloy (a) deformed at 800 °C and solution treated at 800 °C for 1 h and (b) deformed at 650 °C and solution treated at 700 °C for 1 h, followed by furnace cooling and water quenching.

3.2. Elastic modulus

The elastic modulus of the cp-Ti, heat-treated TZN and TNTZ alloys measured by both the techniques is shown in Fig. 6.

The average value of the elastic modulus of cp-Ti obtained by nano-indentation and ultrasonic technique was 119 ± 4.6 and 121 ± 0.87 GPa (Fig. 6a), respectively. On the other hand, TNTZ alloy showed the average elastic modulus value of 57 ± 3.0 and 60 ± 1.9 GPa (Fig. 6a) by nano-indentation and ultrasonic methods, respectively.

Fig. 6b shows the elastic modulus of TZN alloy, furnace cooled and water quenched from 800 °C, measured by both the

techniques. The elastic modulus values of TZN samples furnace cooled and water quenched from 800 °C as measured by the nano-indentation technique was found to be 69 and 65 GPa, respectively, with a variation of up to ± 8 GPa. By comparison, the ultrasonic method gave the elastic modulus of the same samples to be 88 and 61 GPa, respectively, with a variation of up to ± 2.4 GPa.

In case of TZN samples furnace cooled and water quenched from 700 °C, the elastic modulus was 67 ± 6.3 and 70 ± 8.2 GPa, respectively, by the nano-indentation technique and 87 ± 2.5 and 69 ± 0.54 GPa, respectively, by ultrasonic method (Fig. 6c).

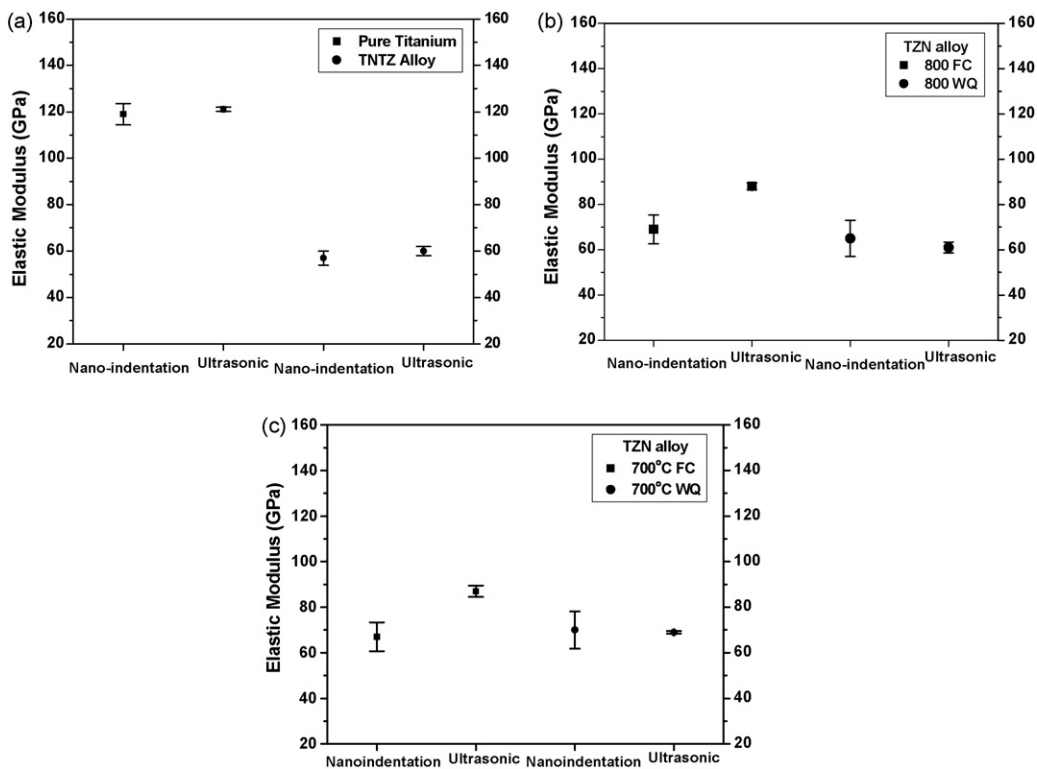


Fig. 6. Elastic modulus of (a) cp-Ti and TNTZ deformed at 850 °C and solution treated at 800 °C for 1 h followed by WQ (b) TZN alloy deformed at 800 °C and solution treated at 800 °C for 1 h followed by furnace cooling and water quenching and (c) TZN alloy deformed at 650 °C and solution treated at 700 °C for 1 h, followed by furnace cooling and water quenching.

The elastic modulus of the cp-Ti obtained by both the techniques is close to the standard value, which is 105 GPa [37]. The elastic modulus of near β TZN alloy is less than that of cp-Ti. In case of β TNTZ alloy, the elastic modulus is about half of the elastic modulus of cp-Ti. Compared with cp-Ti and TZN samples, the elastic modulus of TNTZ alloys is closer to that of the bone (10–40 GPa).

The elastic modulus of stainless steel and Co-based alloys is 206 and 240 GPa, respectively, which is significantly higher than that of bone tissue (\sim 10–40 GPa). The elastic modulus of cp-Ti, near β and β Ti alloys vary between 121 and 57 GPa. The constituent phases of the Ti alloys have different elastic modulus values. It has been reported that the α phase exhibits a much higher elastic modulus as compared with the β phase and the elastic modulus of the phases of titanium alloys increase in the sequence $\beta < \alpha'' < \alpha < \omega$ [1,38,39]. Hon et al. [39] have reported that different phases (α , β and ω) have different elastic modulus and they were found to be related by $E_\alpha = 1.5E_\beta$ and $E_\omega = 2.0E_\beta$. Moreover, Kim et al. [40] have reported that the metastable β phase has lower elastic modulus than stable β phase.

In the present investigation, the cp-Ti consisted of single-phase α (Fig. 1a) and thus, showed higher elastic modulus value than other investigated samples. The microstructure of the TNTZ alloy is mainly single-phase equiaxed β grains (Fig. 2a) and hence it gave the lowest elastic modulus value. The microstructure of TZN alloy water quenched from 800 °C is mainly martensite with some amount of β phase in the matrix (Fig. 3b). The elastic modulus of this sample is 61 GPa (measured by ultrasonic method), which is close to that of β Ti alloy. The other investigated TZN alloys consisted of α and β phases with different morphology and distribution and hence their elastic modulus falls between that of cp-Ti and β Ti alloy.

In nano-indentation technique, the accuracy of the elastic modulus measurement depends on whether the projected area of the indentation is a sufficient sampling area to represent an average elastic modulus. An indentation depth of 2 μm corresponds to a projected triangular area of side \sim 14 μm [15]. The nano-indentation technique should give accurate estimation of the elastic modulus for single-phase materials or for multiphase materials with very fine precipitates distributed homogeneously in the matrix. The large deviation from the average values can be attributed to inhomogeneity in the microstructure on nanoscale. Also, the deviation can be influenced by the position of the indentation. The scatter in elastic modulus measurement with nano-indentation method seems to be inherent in the technique with the scatter being more apparent in case of multiphase material than in the single-phase material. In this study, both cp-Ti and TNTZ consisted of single-phase grains, and hence they showed less scatter in the measured elastic modulus values than multiphase TZN alloy. This is simply because the elastic modulus measurement of a multiphase material by nano-indentation method is strongly influenced by the selection of the location of the indentation in the microstructure, the size of the microstructural constituents and the elastic modulus of the individual phases.

In case of ultrasonic technique, the velocity of ultrasound in materials is generally obtained from the time of flight of ultra-

sonic waves through the known thickness of the sample and it is directly related to the elastic property and density of the solid. Hence, the elastic modulus of the material measured by ultrasonic technique is a better representation of the bulk material property. In case of cp-Ti, TNTZ, and water quenched TZN alloys, the elastic modulus values obtained by nano-indentation and ultrasonic techniques are comparable. At room temperature, the pure cp-Ti exhibits single-phase α structure (Fig. 1a). TNTZ 800 WQ alloy consists of mainly β matrix (Fig. 2a). The overall microstructure of TZN 800 WQ is martensite with a small amount of β phase (Fig. 3b). In case of two-phase α/β TZN alloy water quenched from 700 °C (Fig. 4b), a fine and uniform distribution of α and β throughout the microstructure was observed resulting in more or less similar elastic modulus values by both the techniques.

However, in case of TZN samples furnace cooled from 800 and 700 °C, a large difference was observed in the elastic modulus measured by nano-indentation and ultrasonic techniques. This can be attributed to the non-uniform distribution of the phases in the microstructure. Moreover, the microstructure was relatively coarse in these cases. The TZN sample furnace cooled from 800 °C produced basket-wave type structure characteristic of Widmanstätten structure. Lamellar packets of α grains of different orientations were observed within prior β grains. Presence of primary α phase of globular morphology and transformed β was observed in the TZN alloy furnace cooled from 700 °C. In both these samples, α grains were bigger compared with the indentation area; accordingly, the indentations were mainly taken on the matrix and the large α grains were deliberately avoided in order to obtain the average property of the material. In this process, the elastic modulus of the lamellar and globular α phase, which is higher than that of β phase, was not included into the average elastic modulus value. Hence, the elastic modulus measured by nano-indentation technique is lower than that of ultrasonic method.

4. Summary and conclusions

- (I) The elastic modulus of the investigated Ti and its alloys varies between 60 and 120 GPa. The β TNTZ alloy shows lowest elastic modulus whereas cp-Ti with α grains gives highest elastic modulus among the investigated samples. The elastic modulus of the near β TZN alloy falls in between Ti and TNTZ alloy. Heat treatment of the TZN alloy changes its constituent phases and their size, distribution and morphology. Hence, the elastic modulus also changes accordingly. In general, elastic modulus of the samples water quenched from single-phase or two-phase region is lower than samples furnace cooled from same temperature.
- (II) Elastic modulus can be measured more accurately by ultrasonic method, as it is directly related to the elastic property and density of the material.
- (III) The accuracy of elastic modulus measurement using nano-indentation technique depends on the projected area of indentation. The measurements are expected to be accurate if the indentation samples sufficiently large area to

give adequate representation to all the constituent phases of a material.

References

- [1] Y.L. Hao, M. Niinomi, D. Kuroda, F. Fukunaga, Y.L. Zhou, R. Yang, A. Suzuki, *Met. Mater. Trans. A* 33 (2002) 3137–3144.
- [2] D. Velten, K. Schenk-Meuser, V. Biehl, H. Duschner, J. Breme, *Zeitsch. Metallk. 6* (2003) 667–675.
- [3] M. Niinomi, *Mater. Sci. Eng. A* 243 (1998) 231–236.
- [4] D. Kuroda, M. Niinomi, M. Morinaga, Y. Kato, T. Yashiro, *Mater. Sci. Eng. A* 243 (1998) 244–249.
- [5] H. Kawahara, *Bull. Jpn. Inst. Met.* 31 (1992) 1033–1039.
- [6] F. Widu, D. Drescher, R. Junker, C. Bouraueil, *J. Mater. Sci. Mater. Med.* 10 (1999) 275–281.
- [7] R. Banerjee, S. Nag, J. Stechschulte, H.L. Fraser, *Biomaterials* 25 (2004) 3413–3419.
- [8] S. Nag, R. Banerjee, H.L. Fraser, *Acta Biomater.* 3 (2007) 369–376.
- [9] Y. Okazaki, Y. Ito, A. Ito, T. Tateishi, *Mater. Trans. JIM* 34 (1993) 1217–1222.
- [10] M. Niinomi, D. Kuroda, K.I. Fukunaga, M. Morinaga, Y. Kato, T. Yashiro, A. Suzuki, *Mater. Sci. Eng. A* 263 (1999) 193–199.
- [11] C.W. Lin, C.P. Ju, J.H. Chern Lin, *Biomaterials* 26 (2005) 2899–2907.
- [12] M. Geetha, A.K. Singh, A.K. Gogia, R. Asokamani, *J. Alloys Comp.* 384 (2004) 131–144.
- [13] J.I. Qazi, B. Marquardt, L.F. Allard, H.J. Rack, *Mater. Sci. Eng. C* 25 (2005) 389–397.
- [14] M. Geetha, U.K. Mudali, A.K. Gogia, R. Asokamani, B.D. Raj, *Corros. Sci.* 46 (2004) 877–892.
- [15] S. Nag, R. Banerjee, H.L. Fraser, *Mater. Sci. Eng. C* 25 (2005) 357–362.
- [16] N. Sagaguchi, M. Niinomi, T. Akahori, J. Takeda, H. Toda, *Mater. Sci. Eng. C* 25 (2005) 370–376.
- [17] N. Sagaguchi, M. Niinomi, T. Akahori, J. Takeda, H. Toda, *Mater. Sci. Eng. C* 25 (2005) 363–369.
- [18] M. Ikeda, S.Y. Komatsu, I. Sowa, M. Niinomi, *Met. Mater. Trans. A* 33 (2002) 487–493.
- [19] M. Niinomi, *Biomaterials* 24 (2003) 2673–2683.
- [20] T. Akahori, M. Niinomi, H. Fukui, M. Ogawa, H. Toda, *Mater. Sci. Eng. C* 25 (2005) 248–254.
- [21] M. Niinomi, T. Akahori, T. Takeuchi, S. Katsura, H. Fukui, H. Toda, *Mater. Sci. Eng. C* 25 (2005) 417–425.
- [22] Y. Okazaki, *Curr. Opin. Sol. State Mater. Sci.* 5 (2001) 45–53.
- [23] W.F. Ho, C.P. Ju, J.H. Chern Lin, *Biomaterials* 20 (1999) 2115–2122.
- [24] T. Saito, T. Furuta, J.H. Hwang, S. Kuramoto, K. Nishino, N. Suzuki, R. Chen, A. Yamada, K. Ito, Y. Seno, T. Nonaka, H. Ikehata, N. Nagasako, C. Iwamoto, Y. Ikuhara, T. Sakuma, *Science* 300 (2003) 464–467.
- [25] C. Munuera, T.R. Matzelle, N. Kruse, M.F. Loípez, A. Gutiérrez, J.A. Jiméñez, C. Ocal, *Acta Biomater.* 3 (2007) 113–119.
- [26] S. Mändl, B. Ruschenbach, *Surf. Coat. Technol.* 156 (2002) 276–283.
- [27] B. Gasser, in: D.M. Brunette, P. Tengvall, M. Texfor, P. Thomsen (Eds.), *Titanium in Medicine*, Springer, New York, 2001, pp. 673–701.
- [28] Y. Okazaki, Y. Ito, T. Tateishi, *Mater. Trans. JIM* 37 (1996) 843–849.
- [29] C.M. Lee, W.F. Ho, C.P. Ju, J.H. Chern Lin, *J. Mater. Sci. Mater. Med.* 13 (2002) 695–700.
- [30] S. Dong, B.D. Beake, R. Parkinson, B. Xu, Z. Hu, T. Bell, *Surf. Eng.* 19 (2003) 195–199.
- [31] A.A. Volinsky, W.W. Gerberich, *Microelectron. Eng.* 69 (2003) 519–527.
- [32] M. Long, H.J. Rack, *Wear* 205 (1997) 130–136.
- [33] B. Raj, V. Moorthy, T. Jayakumar, K.B.S. Rao, *Int. Mater. Rev.* 48 (2003) 273–325.
- [34] M. Doghmane, F. Hadjoub, A. Doghmane, Z. Hadjoub, *Mater. Lett.* 61 (2007) 813–816.
- [35] F. Augereau, D. Laux, L. Allais, M. Mottot, C. Caes, *Ultrasonics* 46 (2007) 34–41.
- [36] P. Majumdar, S.B. Singh, M. Chakraborty, *Wear*, in press.
- [37] M. Long, H.J. Rack, *Biomaterials* 19 (1998) 1621–1629.
- [38] R. Banerjee, S. Nag, H.L. Fraser, *Mater. Sci. Eng. C* 25 (2005) 282–289.
- [39] Y.H. Hon, J.Y. Wang, Y.N. Pan, *Mater. Trans.* 44 (2003) 2384–2390.
- [40] H.S. Kim, W.Y. Kim, S.H. Lim, *Scripta Mater.* 54 (2006) 887–891.